

# **A quasi 2-D localized corrosion model**

**Srdjan Nestic and Ying Xiao**

Institute for Corrosion and Multiphase Technology  
340 ½ West State Street, Ohio University, Athens, OH 45701

**B.F.M Pots**

Shell Global Solutions US  
3333 Highway 6 South Houston, TX 77082-3199

## **ABSTRACT**

In 1996 Pots has written a two-dimensional (2-D) stochastic algorithm to simulate the morphology of localized attack. The rule based algorithm operates on the assumption that the morphology of corrosion attack depends on the balance of two processes: corrosion (leading to metal loss) and precipitation (leading to metal protection). The rules of the original algorithm were modified to enable simulation of a broader variety of localized corrosion morphologies found in practice. The algorithm, which uses scaling tendency as the only input parameter, was connected with the mechanistic model of CO<sub>2</sub> corrosion so that the morphology of localized attack can be predicted as a function of primitive parameters such as temperature, pH, partial pressure of CO<sub>2</sub>, velocity, etc.

Based on the results of the simulations, it was postulated that partially protective films are sufficient to trigger localized attack, which is in agreement with the experimental observations.

**Keywords:** localized corrosion, model, stochastic, pitting, iron carbonate, scaling tendency, steel

## **INTRODUCTION**

CO<sub>2</sub> corrosion, or the so called “sweet corrosion”, is a major concern in the application of carbon and low alloy steels, which are still the principal construction materials, offering economy, availability and strength. In practice, localized corrosion is the most dangerous mode of attack and can result in serious failures. Therefore, there is a need to predict the occurrence of localized CO<sub>2</sub> corrosion of carbon and low alloy steels materials.

Significant progress has been made in understanding uniform CO<sub>2</sub> corrosion, and hence some successful uniform corrosion models have been built. However, much less attention has been given to localized CO<sub>2</sub> corrosion and it is still not well understood, and even more difficult to predict or detect comparing to uniform corrosion. Gunaltun<sup>(1)</sup>, in 1996, proposed a localized corrosion prediction model, which applies a turbulence factor to the general corrosion rate, assuming the flow to be the main parameter initiating localized attack. In 1999, Schmitt<sup>(2)</sup>, had developed a probabilistic model for the prediction of flow induced localized corrosion. It is well known however that there are other environmental factors, such as pH, temperature, partial pressure of CO<sub>2</sub><sup>(3)</sup>, etc. causing carbon steel to undergo rapid, localized corrosion, and therefore a model that could predict the localized attack must take all of these into account.

Localized corrosion of metals is stochastic in nature<sup>(4-8)</sup>, and it is believed to relate to two stochastic processes: the breakdown of the passive film and the repassivation of the exposed area<sup>(7, 9-12)</sup>. The probabilistic characters of localized attack make a stochastic approach to its study attractive<sup>(4, 5, 13)</sup>.

## BACKGROUND

In 1996 Pots<sup>(14)</sup> has written a two-dimensional (2-D) stochastic algorithm to simulate the morphology of localized attack. The rule based algorithm operates on the assumption that the morphology of corrosion attack depends on the balance of two processes: corrosion (leading to metal loss) and precipitation (leading to metal protection). This balance has effectively been quantified by van Hunnik *et al*<sup>(14)</sup> using a single parameter: the scaling tendency (ST):

$$ST = \frac{R_{FeCO_3}}{CR} \quad (1)$$

where  $R_{FeCO_3}$  is the precipitation rate of iron carbonate and  $CR$  the corrosion rate, both expressed in the same volumetric units (e.g. mm/y). It has been experimentally observed that if the precipitation rate exceeds the corrosion rate, a protective film forms at the metal surface and the corrosion rate is greatly reduced. On the other hand, if the corrosion rate is much larger than the precipitation rate, protective films cannot form as corrosion creates voids underneath the film faster than precipitation can fill them up. According to a recent experimental study by Sun and Nescic<sup>(3)</sup> there is a “gray zone” in between these extremes where localized corrosion occurs.

Returning to the original Pots<sup>(14)</sup> algorithm, scaling tendency ( $ST$ ), is used as the only input parameter describing the corrosion process. For example, when the  $ST$  is set to zero (meaning that there is no film precipitation), the algorithm predicts uniform corrosion with a constant metal penetration rate as shown in Figure 1. On the other extreme, when the input  $ST$  tendency is set to 1, (which represents the largest value allowed in the algorithm) a protective film is formed very fast, hindering any further corrosion, as shown in Figure 2. When  $ST$  is set somewhere in between, the algorithm predicts qualitatively either an unprotective film and a moderately high corrosion rate for  $ST=0.22$  (see Figure 3) or a partially protective film leading to localized corrosion attack for  $ST=0.37$  (see Figure 4). It should be noted that the prediction is stochastic, i.e. given the same  $ST$  value, the algorithm leads to somewhat different surface morphologies every time the simulation is repeated. Nevertheless, the overall nature of the attack remains the same as illustrated in Figure 1 - Figure 4, where each simulation was repeated twice for each case.

It is remarkable that one can obtain all these various forms of corrosion attack by varying a single parameter, the scaling tendency. Also interesting is the fact that the algorithm captures the experimental behavior reported by Sun and Netic<sup>(3)</sup> related to localized corrosion occurring in the “grey zone” when partially protective films form. In order to understand how this happens, let us now turn our attention briefly to the inner workings of the algorithm.

The core of the algorithm is remarkably simple. The steel is graphically represented by a gray 200×500 pixels rectangular field on the computer screen. Each pixel represents, in a loose sense, a grain of metal. As we are dealing with a two-dimensional (2-D) situation, each grain has four sides that may or may not be exposed to corrosion (top, bottom, left and right). It is assumed that initially the corrosive fluid is present only on the topside of the steel. Once the corrosion simulation is started, the algorithm randomly selects a grain on the metal surface and corrodes it by decreasing the *corrosion index*,  $CI$ , associated with that grain, by an amount, which is linearly proportional to the number of sides,  $\Theta$ , the grain has exposed to the solution. The rule is:

$$CI_{new} = CI_{old} - 4 \Theta \quad (2)$$

According to this rule, the grain which has three sides exposed (has its  $CI$  reduced) corrodes three times faster than the grain with only one side exposed. Initially, all the grains in the top layer have only one side exposed ( $\Theta=1$ ) and all the other internal grains have no exposed sides ( $\Theta=0$ ). This changes as the simulation progresses and the grains get corroded away. If it happens that all the grains around a particular grain corrode away, that grain with  $\Theta=4$  becomes detached and is removed from the simulation. Every grain starts out with the same, arbitrarily chosen, corrosion index,  $CI=10$ , and is corroded away when  $CI$  decreases to or below zero. When this happens, the corresponding steel pixel is removed from the simulation while on the screen it changes its color from gray to blue.

In the simulation, precipitation of a film happens alongside with corrosion, in alternating steps. The algorithm performs the precipitation step by randomly selecting a grain where precipitation will happen. Precipitation is simulated by increasing a film index,  $FI$ , for that particular grain. Every grain starts out without any film,  $FI=0$ , and if hit by precipitation increases its film index until  $FI \geq 10$  when it is considered that that particular grain has a very dense film and is fully protected from corrosion. On the screen this is denoted by a pixel above the protected pixel turning red. Every time the precipitation process randomly “hits” a grain, its film index increases by an amount which is proportional to the number of sides,  $\Theta$ , which that particular grain has exposed to the solution and the scaling tendency,  $ST$ . The rule is:

$$FI_{new} = FI_{old} + 8 \Theta ST \quad (3)$$

Obviously when there is no precipitation ( $ST=0$ ), the film index  $FI$  will not change during the simulation and vice versa when the precipitation rate is high ( $ST \approx 1$ ), the film index for any particular grain will rapidly reach (in one or two hits) the maximum value of 10 when the film is considered to be fully protective.

The simple algorithm described above works remarkably well and produces a wide range of corrosion surface morphologies as already illustrated in Figure 1 - Figure 4. Even though there is not much physico-chemical content built into the algorithm, the appearance of the 2-D corroded surface, including the one with localized attack, is rather similar to what is seen in Scanning Electron Microscope (SEM) images of corroded steel samples. This leads us to a suggestion that in order to get localized attack it is sufficient to have a partially protective film and stochastic corrosion and

precipitation processes. On a microscopic level both the corrosion and the precipitation processes are stochastic in nature, due to a constant interchange of cathodes and anodes, inhomogeneous steel surface metallurgy, stochastic nature of the diffusion process, to name just a few arguments. Therefore one can conclude that all one needs to get localized attack are partially protective films, which is the same conclusion Sun and Nescic<sup>(3)</sup> reached by analyzing long-term CO<sub>2</sub> corrosion experiments in wet gas flow. It can be argued that this is a “minimum requirement” for localized corrosion, notwithstanding the fact that other factors such as hydrodynamics, steel composition, inclusions, etc. might complicate the situation further.

Let us recall that the algorithm requires only one input: the scaling tendency  $ST$ . This apparent strength is its weakness as well, since knowing  $ST$  is not straightforward.  $ST$  depends on the precipitation rate as well as the corrosion rate as shown by equation (1). Neither of the two is easy to predict as they depend on many factors including water chemistry, steel composition, surface electrochemistry, transport of species in the solution, etc. Therefore, given that one knows the primitive input parameters such as temperature, pH, velocity, etc., a model is needed to predict the corrosion and precipitation rates, before  $ST$  can be found.

The second weakness of the original algorithm lies in the arbitrariness of the constants used in the rules expressed above. The constants in equations (2) and (3) have been adjusted relative to each other to give plausible answers in terms of morphology of the corrosion attack. However, the answer is qualitative and cannot be used to deduce the magnitude of the attack, be it uniform or local.

Both weaknesses can be eliminated by linking the algorithm with a corrosion/precipitation model that can predict the scaling tendency  $ST$  and help quantify the magnitude of the attack. For this purpose, the mechanistic one-dimensional (1-D) CO<sub>2</sub> corrosion model of Nescic *et al.*<sup>(15)</sup> has been used as discussed below. Due to this combination of the 1-D mechanistic corrosion model and the 2-D original algorithm, the integrated model was labeled “quasi two-dimensional”, as indicated in the title of the present paper.

## MODEL DEVELOPMENT

Before any linkage with a corrosion/precipitation model was done, the rules of the original algorithm were scrutinized and modified as discussed below.

### Modification of the rules

In the original algorithm, the rate of corrosion of any particular grain on the steel surface is proportional to its exposed surface area. In terms of the rules defined above, the decrease of the corrosion index  $CI$  is only proportional to the number of sides  $\Theta$ , which that particular grain has exposed to the solution (see equation 2). However, the corrosion rate of any particular grain should also be related to the presence of a protective film. The algorithm described above takes this into account only in a crude sense, i.e. when the film index,  $FI$ , increases to or above 10, the grain is considered fully protected and cannot be corroded further. What the original algorithm does not take into account is the effect of partially protective films. We know that surface films range in protectiveness from unprotective to mildly and very protective depending on their density/porosity. This can easily be accommodated by the rules above as the film index,  $FI$ , which varies from 0 to 10, can be seen as an indicator of film protectiveness. We can assume that: the higher the  $FI$  is for a particular grain, the slower it should corrode. Therefore equation (2) can be modified to read:

$$CI_{new} = CI_{old} - 8 \Theta \left( 1 - \frac{FI}{10} \right) \quad (4)$$

When there is no film, i.e. for the grain  $FI=0$ , equation (4) works in the same way as equation (2). However as the grain  $FI$  increases, due to buildup of a protective film, the change in the grain  $CI$ , i.e. its corrosion rate, slows down. Eventually, when the film becomes fully protective (the grain  $FI=10$ ), corrosion is hindered and equation (4) predicts that the grain  $CI$  stops decreasing. In other words, the modification makes the new algorithm work like the original one, at the extremes (no-film and fully protective film situations) and adds the intermediate effect of partially protective films. Note that the constant that determines how fast a particular grain corrodes has been increased from 4 in equation (2) to 8 in equation (4) to balance the additional film-related term which was added.

The effect of the modified rules on localized attack is seen in Figure 5. A larger variety of surface morphologies are now obtained over a broader range of  $ST$ . Pits which narrow toward the bottom as well as “mushroom” style pits appear at various  $ST$ . In certain cases, pits propagate much deeper and even fail to heal.

Comparison of the various steel surface morphologies obtained in the simulations and selected SEM images taken from a  $CO_2$  corrosion study in multiphase flow by Nescic and Lunde<sup>(16)</sup> (see Figure 6. SEM images of the corroded steel surfaces taken from the study of  $CO_2$  corrosion in multiphase flow taken from the study by Nescic and Lunde<sup>(16)</sup>.) clearly confirm that the algorithm discussed above is capable of predicting qualitatively a wide range of localized attack morphologies seen in practice.

### **Link with 1-D Ohio University Corrosion Model**

For the purposes of connecting with the algorithm described above, one needs to compute the scaling tendency at the steel surface where the films form. Therefore one needs information about the solution chemistry at the steel surface, which can be very different from the one in the bulk, particularly if some sort of surface film is already in place (e.g. iron carbide, mill scale). Further, the scaling tendency changes with time as the corrosion and precipitation rate change. Very few corrosion/precipitation models can satisfy this requirement.

The recent 1-D mechanistic model of Nescic *et al.*<sup>(15,17,18)</sup> is a perfect candidate for linkage with the 2-D algorithm described above as it computes concentration profiles of all species involved in the corrosion/precipitation reactions. The model covers most of the important processes present in uniform  $CO_2$  corrosion of carbon steel:

- electrochemical reactions at the steel surface,
- chemical reactions including precipitation and
- transport of species between the steel surface and the bulk solution including transport through the porous corrosion film.

The physical, mathematical and numerical aspects of the model are explained in detail in the original papers,<sup>(15,17,18)</sup> however a very brief outline is given below to facilitate the understanding of the text to follow. Since it is a model of uniform corrosion, a one-dimensional computational domain is used, stretching from the steel surface through the pores of a surface film and the mass transfer boundary layer, ending in the turbulent bulk of the solution, as sketched in Figure 7. The concentration of each species is governed by a species conservation (mass balance) equation. A universal form of the equation

which describes transport for species  $j$  in the presence of chemical reactions, which is valid both for the liquid boundary layer and the porous film, is:

$$\underbrace{\frac{\partial(\varepsilon c_j)}{\partial t}}_{\text{accumulation}} = \underbrace{\frac{\partial}{\partial x} \left( \varepsilon^{1.5} D_j^{\text{eff}} \frac{\partial c_j}{\partial x} \right)}_{\text{net flux}} + \underbrace{\varepsilon R_j}_{\substack{\text{source or sink} \\ \text{due to chemical reactions}}} \quad (5)$$

where  $c_j$  is the concentration of species  $j$  in  $\text{kmol m}^{-3}$ ,  $\varepsilon$  is the porosity of the film,  $D_j^{\text{eff}}$  is the effective diffusion coefficient of species  $j$  (which includes both the molecular and the turbulent component) in  $\text{m}^2 \text{s}^{-1}$ ,  $R_j$  is the source or sink of species  $j$  due to all the chemical reactions in which the particular species is involved in  $\text{kmol m}^{-3} \text{s}^{-1}$ ,  $t$  is time and  $x$  is the spatial coordinate in  $\text{m}$ . It should be noted that in the transport equation above electromigration has been neglected as its contribution to the overall flux of species is small. Turbulent convection has been replaced by *turbulent diffusion* as the former is difficult to determine explicitly in turbulent flow.

One equation of the form (5) is written for each species. They all are solved simultaneously in space and time. The boundary conditions for this set of partial differential equations are: in the bulk - equilibrium concentrations of species (which is also used as the initial condition), and at the steel surface - a flux of species is determined from the rate of the electrochemical reactions (zero flux for non-electroactive species). Once the set of equations is solved in any given time step, the corrosion rate,  $CR$ , can be simply calculated as the flux of  $Fe^{2+}$  ions at the metal surface.

Solid iron carbonate ( $FeCO_3$ ), which is treated as one of the species, will precipitate when the iron carbonate saturation exceeded according to:



The rate of precipitation  $R_{FeCO_{3(s)}}$  in equation (6) can be described as a function of supersaturation  $S$ , the solubility limit  $K_{sp}$ , temperature  $T$  and surface area-to-volume ratio  $A/V$ :

$$R_{FeCO_{3(s)}} = \frac{A}{V} \cdot f(T) \cdot K_{sp} \cdot f(S) \quad (7)$$

Supersaturation is defined as:

$$S = \frac{c_{Fe^{2+}} \cdot c_{CO_3^{2-}}}{K_{sp}} \quad (8)$$

From the two different expressions describing the kinetics of iron carbonate precipitation proposed by Johnson and Tomson<sup>19</sup> and Van Hunnik et al.<sup>(14)</sup>, the latter is used because it is believed to give more realistic results especially at higher supersaturation.

Once the rate of precipitation,  $R_{FeCO_{3(s)}}$ , and the corrosion rate,  $CR$ , are calculated as a function of the input parameters such as temperature, pH, partial pressure of  $CO_2$ , velocity, etc., the scaling tendency  $ST$  can be computed according to equation (1) and used as an input into the algorithm.

An illustration of the integrated quasi 2-D model at work is shown in Figure 8. Under those conditions one gets a very protective film at pH6.6, only a partially protective film and some initial localized attack (which heals) at pH6.3, poorly protective film and progressive localized attack is obtained at pH6.26 while unprotective films and uniform attack is seen at pH6.2 and lower.

## CONCLUSIONS

- The original two-dimensional (2-D) stochastic algorithm by Pots *et al.*<sup>(14)</sup> was modified to enable simulation of a broader variety of localized corrosion morphologies found in practice.
- Based on the results of the simulations, it was postulated that partially protective films are all that is needed to trigger localized attack, which is in agreement with the experimental study of Sun *et al.*<sup>(3)</sup>.
- The original Pots *et al.*<sup>(14)</sup> algorithm, which uses scaling tendency as the only input parameter, was connected with the mechanistic model of Nescic *et al.*<sup>(15,17,18)</sup>, so that the morphology of localized attack can be predicted as a function of primitive parameters such as temperature, pH, partial pressure of CO<sub>2</sub>, velocity, etc.

## FUTURE WORK

- Refine the rules of the algorithm to give even more realistic localized corrosion morphologies.
- Improve the connection between the algorithm and the mechanistic model of Nescic *et al.*<sup>(15,17,18)</sup> so that the likelihood and magnitude of localized attack can be predicted.
- Merge the algorithm with the mechanistic model by extending the latter to two dimensions and introducing the stochastic element to the corrosion and precipitation processes.

## ACKNOWLEDGEMENTS

The authors would like to acknowledge the contribution of the consortium of companies whose financial support was instrumental in providing a scholarship for Y. Xiao. They are BP, ConocoPhillips, ENI, Petrobras, Saudi Aramco, Shell, Total, Champion Technologies, Clariant, MI Technologies and Nalco.

## REFERENCES

1. Y. M. Gunaltun, CORROSION/96, Paper No. 27, NACE International, Houston, Texas, 1996.
2. G. Schmitt, C. Bosch, M. Mueller, G. Siegmund, CORROSION/ 2000, Paper No. 49, NACE International, Houston, Texas, 2000.
3. Y. Sun, K. Gorge, S. Nescic, CORROSION/2003, Paper No. 3327, NACE International, Houston, Texas, 2003.
4. D. E. Williams, C. Westcott, M. Fleischmann, J. Electroanal. Chem., 1984, 180, 549.
5. D. E. Williams, C. Westcott, and M. Fleischmann, J. Electrochem. Soc., 1985, 132, 1796.
6. C. Gabrielli, F. Huet, M. Keddam, R. Oltra, Corrosion, 1990, 46, 266.
7. U. Bertocci, M. Koike, S. Leigh, F. Qiu, G. Yang, J. Electrochem. Soc., 1986, 133, 1782.
8. B. Wu, J. R. Scully, J. L. Hudson, J. Electrochem. Soc., 1997, 144, 1614.

9. M. Hashimoto, S. Miyajima, T. Murata, *Corrosion Science*, 1992, 33, 885.
10. L. Stockert, H. Bohni, *Master. Sci. Forum*, 1989, 44-45, 313.
11. P.C. Pisdrius, G. T. Burstein, *Philos. Trans. R. Soc. Lond.*, 1992, A341, 531.
12. C. Gabrielli, M. Keddam, *Corrosion*, 1992, 48, 794.
13. U. Bertdcci, F. Huet, *Corrosion*, 1995, 51, 131.
14. E.W.J. van Hunnik, B.F.M. Pots, *CORROSION/96*, Paper No. 6.
15. S. Nestic, K. J. Lee, *Corrosion Science*, 2003, 59,616.
16. S. Nestic, L. Lunde, *Corrosion*, 1994, 50,717.
17. S. Nestic, M. Nordsveen, R. Nyborg, A. Stangeland, *Corrosion Science*, 2003, 59,489.
18. S. Nestic, J. Postlethwaite, S. Olsen, *Corrosion Science*, 2003, 52,280.
19. M. L. Johnson, M. B. Tomson, *Corrosion/1991*, Paper No. 268, NACE International, Houston, Texas, 1991.



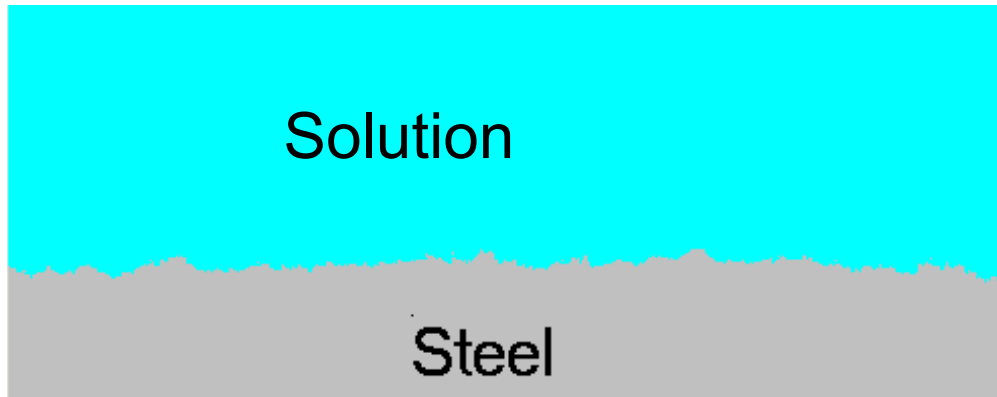


Figure 1. Two samples of simulated metal surface morphology following rapid uniform corrosion without any film precipitation. Original Pots<sup>(14)</sup> algorithm was used.

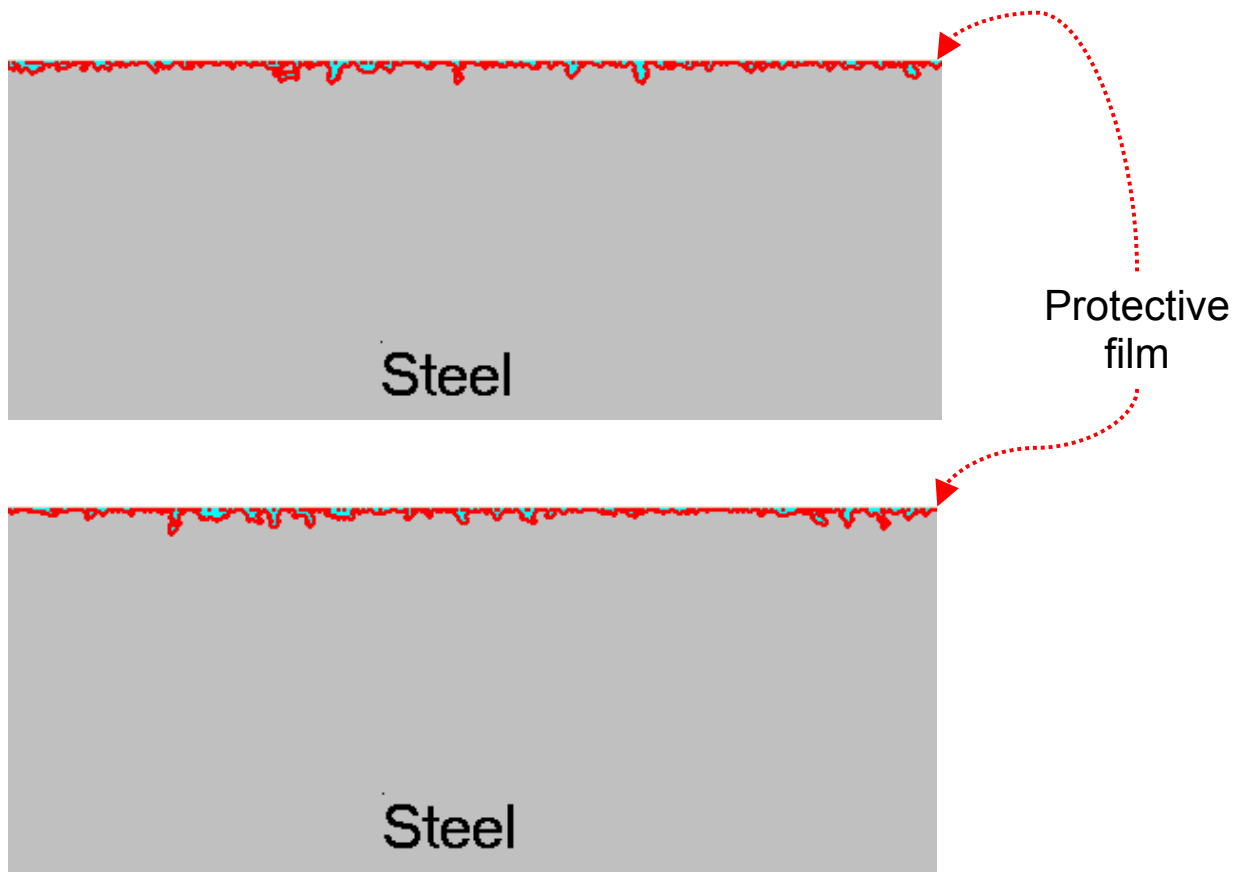


Figure 2. Two samples of the simulated metal surface morphology following rapid precipitation leading to a protective film and very little corrosion. Original Pots<sup>(14)</sup> algorithm was used.

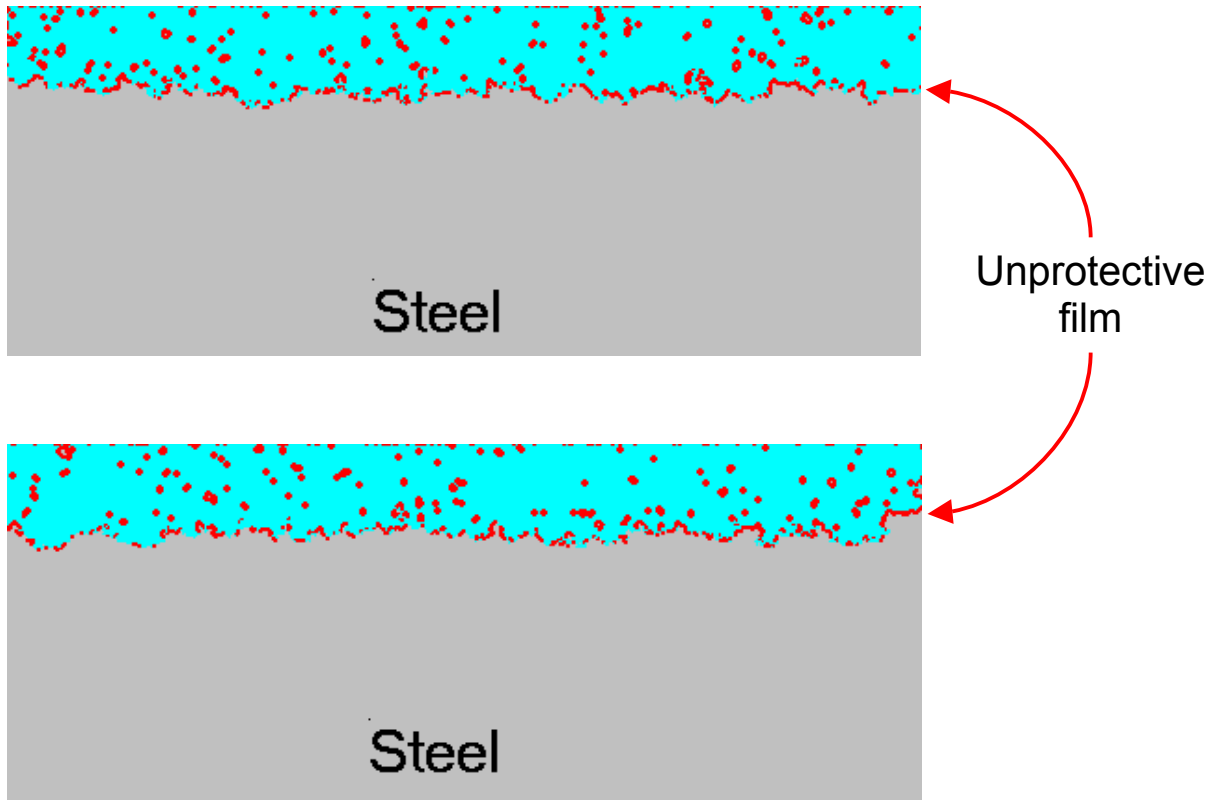


Figure 3. Two samples of simulated metal surface morphology following slow precipitation leading to an unprotective film and a moderate corrosion rate. Original Pots<sup>(14)</sup> algorithm was used.

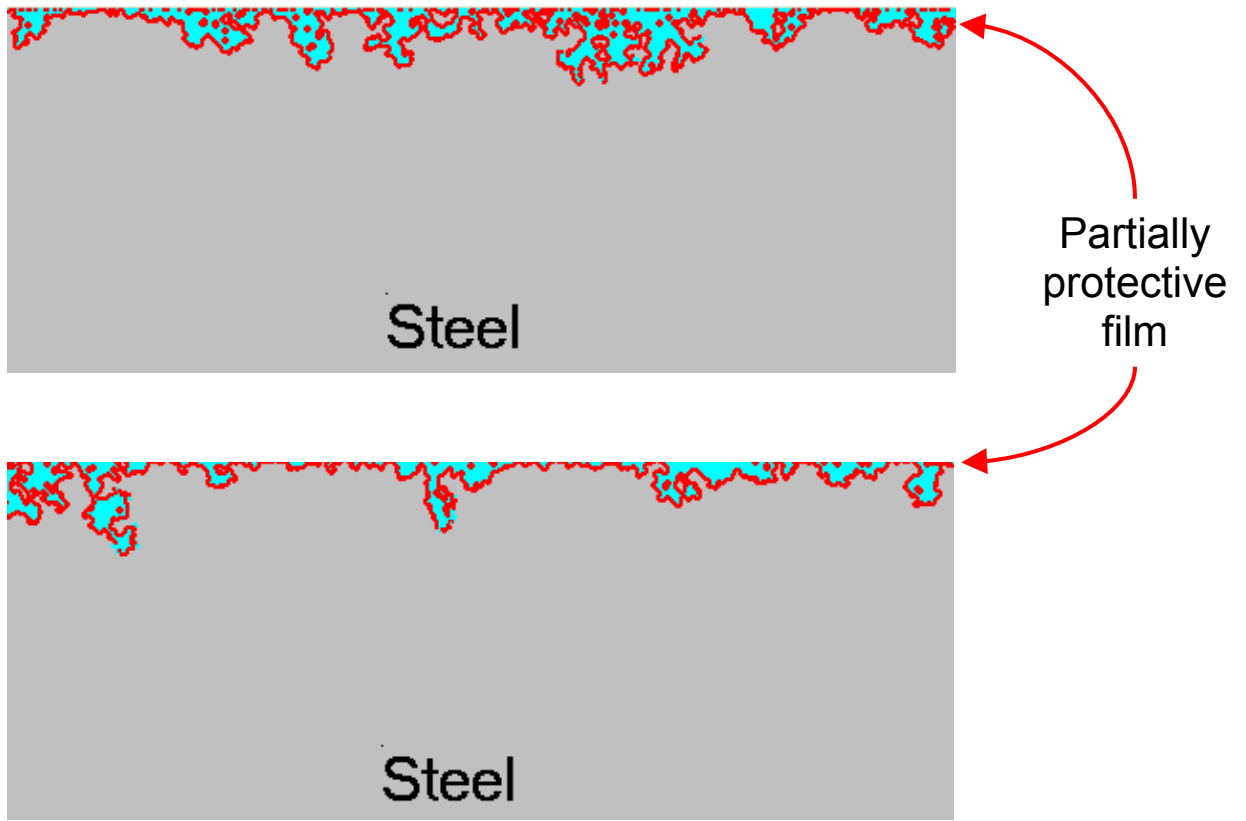
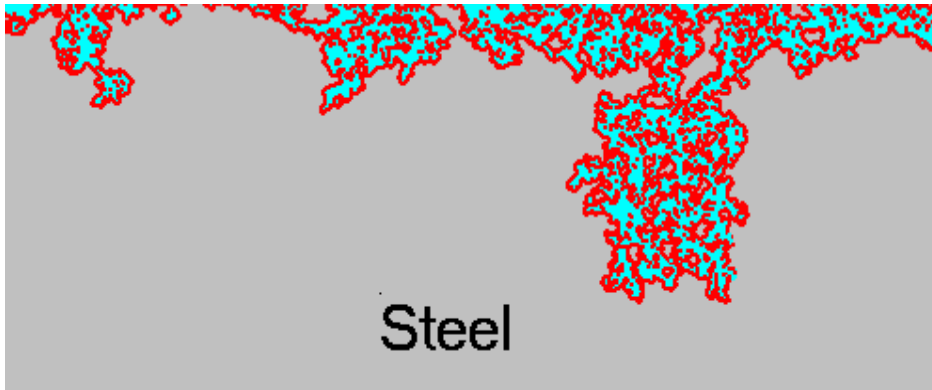
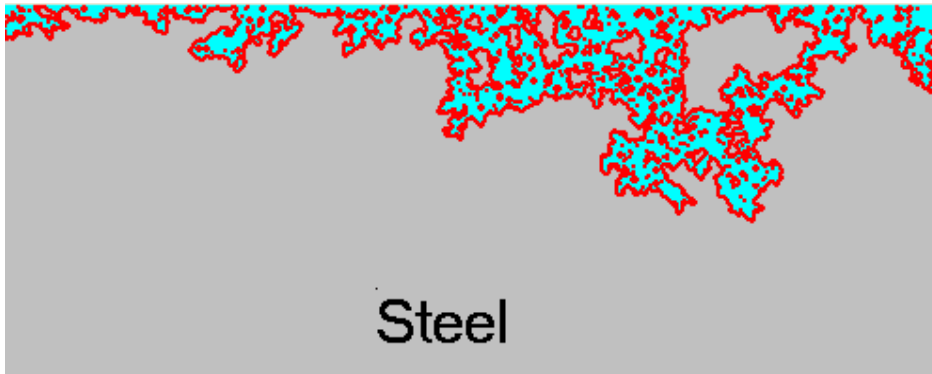


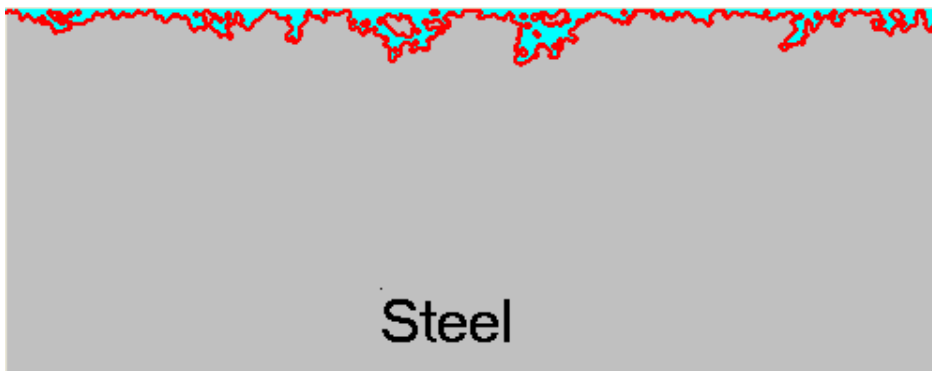
Figure 4. Two samples of simulated metal surface morphology following moderate precipitation leading to a partially protective film and localized corrosion. Original Pots<sup>(14)</sup> algorithm was used.



$ST = 0.45$



$ST = 0.53$



$ST = 0.57$

Figure 5. Three samples of a simulated metal surface morphology following moderate precipitation leading to a partially protective film and localized corrosion. The modified algorithm (equation 4) was used.

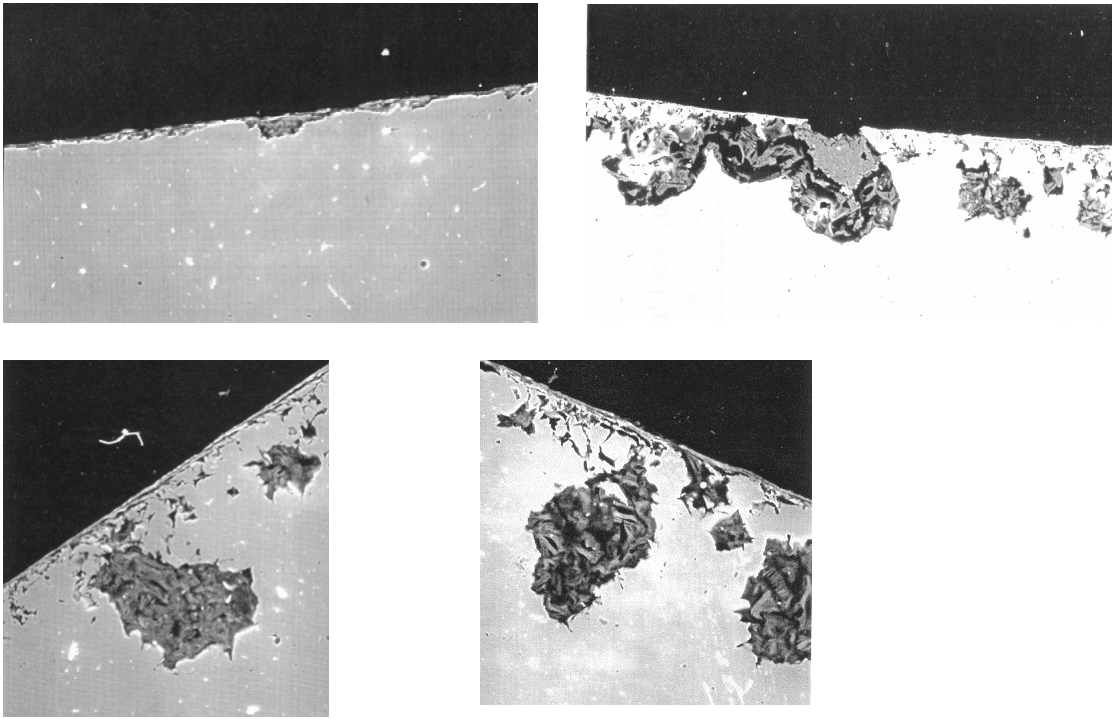


Figure 6. SEM images of the corroded steel surfaces taken from the study of CO<sub>2</sub> corrosion in multiphase flow taken from the study by Nesic and Lunde<sup>(16)</sup>.

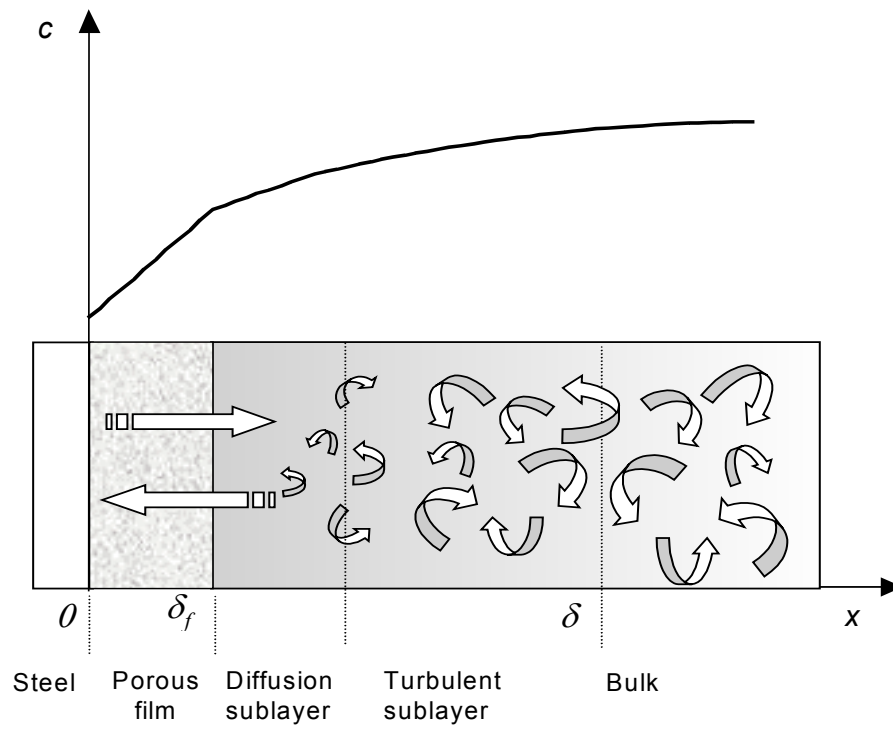


Figure 7. Sketch of the computational domain and a typical concentration profile for a dissolved species.

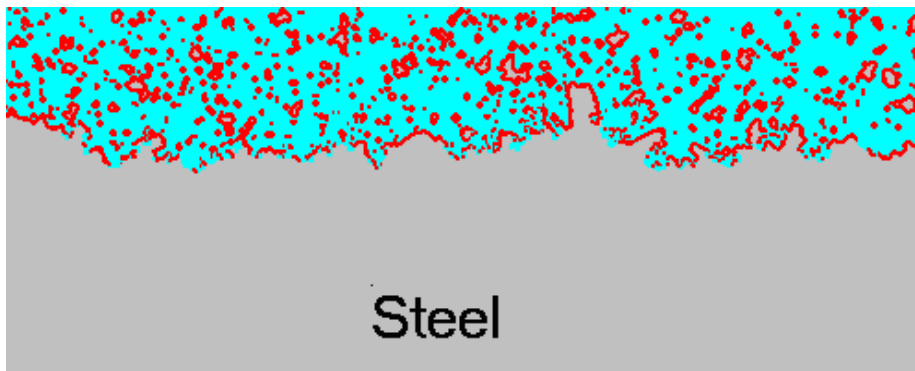
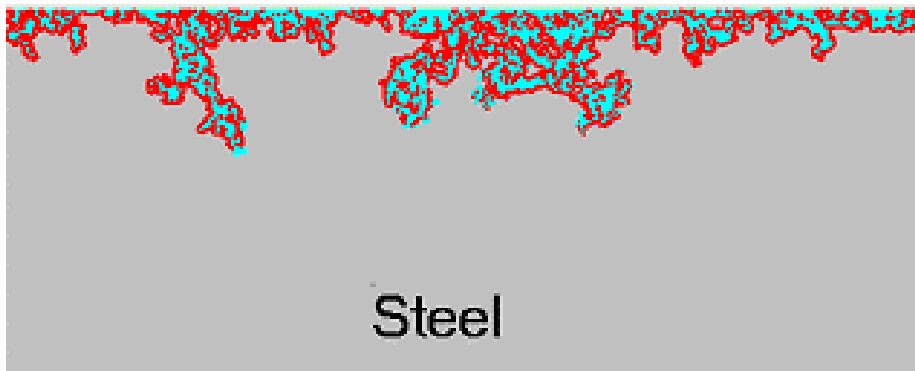
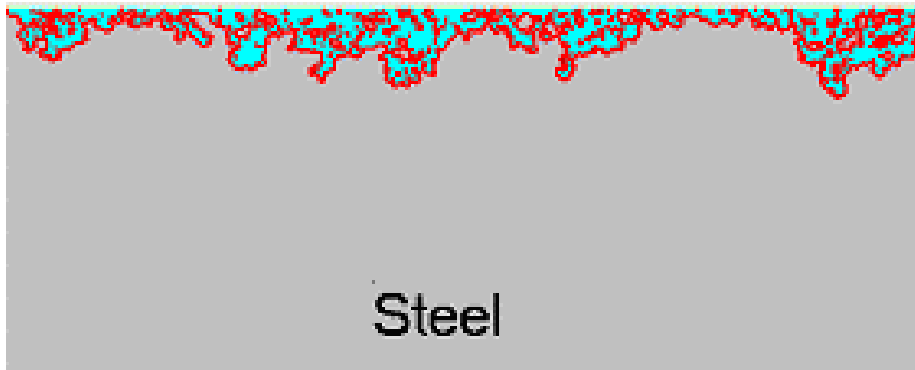
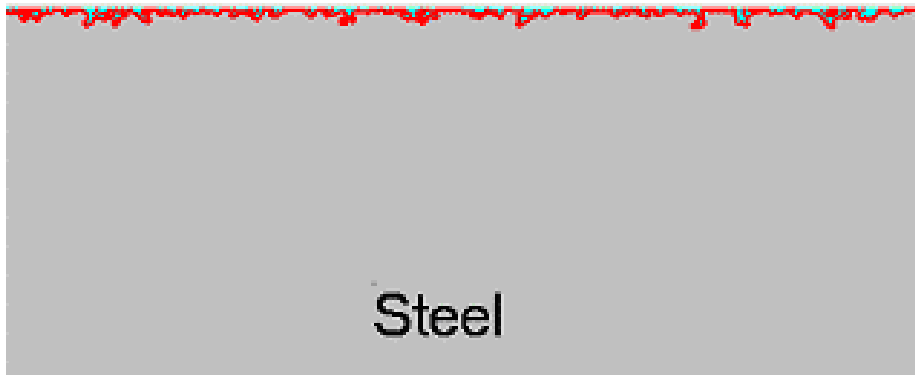


Figure 8. Predictions for the case of a 1%NaCl solution, at  $T = 80^{\circ}\text{C}$ ,  $P_{\text{CO}_2} = 0.52\text{bar}$ ,  $P_{\text{total}} = 1\text{bar}$ ,  $C_{\text{Fe}^{2+}} = 100\text{ppm}$ ,  $v=1\text{ m/s}$ .